Highlights

A novel multi-objective method with online Pareto pruning for multi-year optimization of rural microgrids

Marina Petrelli, Davide Fioriti, Alberto Berizzi, Cristian Bovo, Davide Poli

- Multi-objective multi-year planning of a rural hybrid power system.
- Evaluation of Net Present Cost, CO2 emissions, land use, job creation and public lighting coverage.
- Development of Advanced-AUGMECON2 (A-AUGMECON2) for skipping redundant iterations.
- Multi-year optimization including demand growth, assets degradation and variable efficiency of the battery.
- Application to rural electrification in Soroti, Uganda, Sub-Saharan Africa.

A novel multi-objective method with online Pareto pruning for multi-year optimization of rural microgrids

Marina Petrelli[a,*], Davide Fioriti[b], Alberto Berizzi[a], Cristian Bovo[c], Davide Poli[b]

[a] *Politecnico di Milano, Energy Department, Via Giuseppe La Masa 34, Milano, Italy*
[b] *Università di Pisa, Department of Energy, Systems, Territory and Construction Engineering, Via Carlo Francesco Gabba 22, Pisa, Italy*
[c] *Università di Pavia, Facoltà di Ingegneria, Via Adolfo Ferrata 5, Pavia, Italy*

Abstract

Decentralized hybrid energy systems are promising long-lasting solutions to support local socio-economic development in compliance with environmental concerns. Traditionally, microgrid planning has mainly focused on economics only, sometimes with reliability or environmental concerns, and the project costs have been estimated by approximating the multi-year operation of the system with a single-year approach, thus neglecting assets degradation and demand growth. In this paper, we propose a multi-objective multi-year method to plan microgrid projects in the Global South, accounting for socio-economic, security and environmental impacts on the local community; the entire multi-year lifespan of the project is considered, including detailed degradation of the system assets. In order to solve the proposed non-linear multi-objective model, the advanced version of the augmented ε-constraint algorithm, denoted as A-AUGMECON2, is here proposed, by using a novel pruning algorithm that avoids solving redundant optimizations. The proposed multi-objective multi-year methodology is applied to the numerical case study of an isolated hybrid microgrid in Uganda. Results confirm that the proposed approach successfully quantifies the trade-off between local long-term impacts, namely Net Present Cost, carbon emissions, land use, job creation, and public lighting coverage, in terms of the Pareto-optimal designs, which can successfully support policy makers and local developers in devel-

*Corresponding author
Email address: marina.petrelli@polimi.it (Marina Petrelli)

oping effective policies and projects. Moreover, the novel A-AUGMECON2 algorithm enables reducing by 48% the computational requirements of the standard AUGMECON2, which extends the application of multi-objective methodologies to more complex problems.

Keywords:
Hybrid microgrid sizing, Mixed-Integer Linear Programming (MILP), eps-constraint method, online Pareto filter, holistic design, off-grid systems

---

1. Introduction

1.1. Motivation

As stated in the Sustainable Development Goals, achieving universal electricity access is a key priority of the international community [1]. Electricity is a well-known determinant for social development [2], as it enables the use of modern appliances, replaces lower quality energy sources, such as kerosene, wood, and charcoal, stimulates economic growth, and improves well-being [3, 4], given the possible synergies with access to food and water under the water-energy-food nexus [5].

However, currently, almost 800 million people live without access to electricity, and most of them are located in rural areas in Sub-Saharan Africa [6], which are often difficult to reach. Additionally, these remote areas typically rely on subsistence economy, with very basic electricity needs, such as lighting and charging of mobile phones; therefore, depending on the location, extending the public power grid may be considered too expensive and not-worth in the short-term. Conversely, decentralized solutions such as microgrids can be promising and cost-effective solutions, but adequate optimization tools shall be developed to account for the multi-faceted context of rural areas in the Global South for the entire lifetime of the project.

Given the strong recent efforts by governments and international entities in addressing the rural electrification challenge, it is timely and useful to develop a multi-objective planning methodology able to address economic, social, and environmental objectives, besides accounting for the entire multi-year simulation of the project lifetime and including the degradation model of the assets. On the other side, in order to tackle the increased complexity in the planning methodologies, it is also important to develop novel techniques to more efficiently address multi-objective optimization, as proposed in this

study. The multi-objective planning of rural microgrids, here formulated using Mixed-Integer Linear Programming (MILP), is successfully solved in this paper by developing the novel A-AUGMECON2 method, that is an improved version of the standard augmented ε-constraint method [7, 8], to efficiently deal with the multi-objective optimization and reduce computational requirements without affecting the quality of the results.

1.2. Literature analysis

Standard microgrid sizing tools usually focus on single-year economics-only optimizations in order to reduce the complexity of the analysis. In [9–11], the least-cost solution, in compliance with the technical features of the components, is identified by optimizing the generating portfolio together with the scheduling strategy of the first year, assumed to be representative of all the subsequent years. Likewise, the operating costs will also recur from year to year. Therefore, cost is considered as the only determining factor in the effectiveness of the rural electrification process. These assumptions hardly match the complex circumstances of off-grid microgrids in the Global South, given the multiplicity of impacts on the community involved, the intrinsic long-lasting nature of the system, the significant load growth and the assets degradation over the years. Neglecting these aspects in favour of more details on short-term features can lead to sub-optimal designs, since long-term dynamics are more relevant in rural contexts and significantly affect the optimal choice of the system [12].

Only few studies have recently adopted a multi-year approach, partially integrating the multi-year characteristics of the system [13–15]; namely, load growth [13, 15] and storage capacity reduction, regardless of how the batteries are used [14, 15]. Actually, the pace at which batteries degrade is strongly linked to their operation [16] and this has significant impact on the optimal microgrid planning and scheduling [17]. Moreover, renewable energy generators are subject to performance deteriorations too [18, 19], and this influences their optimal size.

A growing interest in environmental protection issues has led various scholars to also include an assessment of carbon emissions in their analyses, as a limit not to be exceeded [20], or as monetary cost to be minimized [15, 21], or as additional objective function [22–25]; however, Life-cycle Assessment (LCA), which quantifies the emissions along the whole life-cycle of an asset, is rarely adopted [20, 24], and generally only direct emissions are

taken into account [15, 21–23, 25], resulting in incomplete and sometimes misleading evaluations.

In addition to this, the importance of considering the social impact of rural electrification projects is increasingly recognized and demanded as an indispensable element of system planning tools [26]. Nonetheless, very few multi-objective algorithms have been developed including social assessments. The most common social aspect under analysis is the employment generation [27–29], while the maximization of the Human Development Index (HDI) in relation to energy consumption is rarely adopted [29]. Although the relationship between HDI and energy use is widely recognized nowadays, it can hardly describe the local impact on the electrified community, while job creation is an understandable and measurable criterion in situ; this is why the latter is used much more extensively.

A popular and consolidated approach for holistic analysis of rural electrification projects is to use Multi-Criteria Decision Analysis (MCDA) [30–33], which is more prone to including social and qualitative decision criteria. However, MCDA cannot determine the generation mix and the scheduling strategy and is not able to efficiently manage different configurations of hybrid systems. Hence, these aspects must be analysed separately and MCDA is used for ex-ante [32] or ex-post [33] assessments, but planning tools are still needed.

Therefore, it turns out that the literature lacks a holistic multi-objective optimization that addresses all the aforementioned shortcomings.

In the scope of MILP optimization, the most common approaches to solve multi-objective problems are the weighted sum method [34, 35] and the ε-constraint method [36–38]. The latter has the advantage of being able to represent the entire Pareto frontier independently of its shape; moreover, its results are not influenced by normalization issues and it generally has better computational performances [39, 40]. In particular, the augmented ε-constraint method (AUGMECON2) has been developed as an advancement of the traditional ε-constraint method [7, 8] and, currently, it is a well consolidated method, widely adopted to solve a diverse portfolio of problems in the energy sector [37, 38, 41, 42].

However, AUGMECON2 presents two interrelated drawbacks: 1) when complex algorithms with more than two objective functions are optimized, the computational burden may become extremely large because of the presence of redundant iterations; 2) the higher the desired resolution of the Pareto frontier, the more the redundant points. The former issue needs an advance-

ment of the methodology, while the latter, which is related to the readability of the results and the choice of the final point, could be faced by one of the post-Pareto selection methods available. These can be grouped into three major categories: offline pruning algorithms to reduce the number of Pareto points [43, 44]; clustering algorithms to identify and group similar solutions [45]; mathematical methods to select a single final point [46, 47]. This additional step requires further computational resources, thus exacerbating the first issue.

AUGMECON2 is selected by the authors to solve the multi-objective multi-year optimization under study, and its two main shortcomings are faced by a novel methodology, aimed at providing better computational performances and improved readability of the Pareto frontier by means of an online filter of redundant optimizations.

1.3. Contributions

To the best of the authors' knowledge, this is the first study discussing the multi-objective multi-year planning of an off-grid microgrid, accounting for its entire lifetime by using a modified version of AUGMECON2, here denoted as A-AUGMECON2. The proposed approach, which is firstly presented in this paper, goes beyond the state of the art because it preemptively detects the redundant simulations, thus reducing the computational requirements without affecting the quality of the results. The assets degradation and their operational constraints have been taken into account by using a custom iterative approach that enables decomposing the general non-linear problem into the consecutive optimization of simple MILP problems, where constant parameters are updated in every iteration [17]. Economic (Net Present Cost), social (Job Creation and Public Lighting), and environmental (Life-cycle emissions and Land use) concerns are considered as objective functions. In short, the main novelties are discussed below.

1. Development of a multi-objective multi-year planning methodology able to efficiently optimize and simulate the operation of the entire lifetime of a project, using economic, social, and environmental objective functions.
2. Detailed modelling of the degradation of the assets of the microgrid performed by decomposing the full non-linear model into the iterative optimization of a MILP problem.

3. Development of the A-AUGMECON2 methodology that reduces the computational requirements of the standard AUGMECON2, using a novel pruning algorithm that avoids the simulation of redundant iterations and enables the introduction of the first two novelties while keeping a good tractability of the algorithm.

2. Microgrid planning

In this section, the model for the multi-year planning of off-grid microgrid projects is described. The formulation, based on [17], accounts for detailed hourly simulations of the entire lifetime of the microgrid project, including the operational effects of the generation and storage degradation.

2.1. Description

The configuration of the microgrid considered in this study and shown in Figure 1 is aimed at representing the typical off-grid system in the Global South: it includes photovoltaic panels of type p, wind turbines of type w, fuel-fired generators of type g), and battery storage of type b, coupled at the AC busbar to supply the demand. The elements in the set $i \in \{p, w, g, b\}$ represent the different technologies available for each asset.

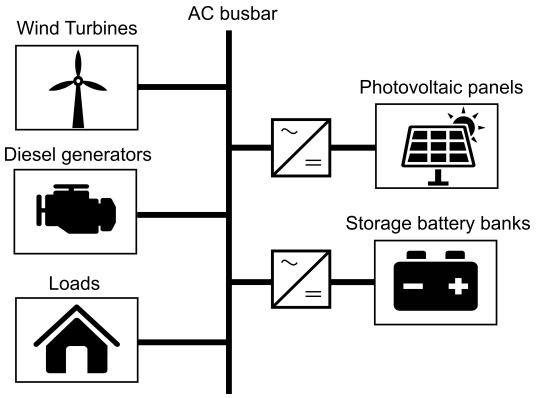

Figure 1: Microgrid architecture [17].

The proposed model aims at reproducing the design and dispatch of the system at every hour of the project lifetime, typically lasting several years, also accounting for the degradation of the main assets.

2.2. The objective functions

While the scientific literature devoted to the optimal microgrid sizing has widely focused only on economics, the following socio-economic and environmental objectives are considered in this work: Net Present Cost, life-cycle emissions, land usage, job creation and public lighting supply. Their mathematical formulation is discussed in the following subsections.

2.2.1. Net Present Cost

As typically done in microgrid investments [17], Net Present Cost is considered as economic objective function, to be minimized, according to the mathematical description detailed in (2)-(8). Its formulation takes into account the investment costs (IC_i) of every component $i \in \{p, w, g, b\}$, the operation and maintenance charges ($O\&M_i$), the replacement costs RC_i of batteries and diesel generators, and the residual values RV_i of the assets at the end of the project lifetime. In particular, IC_i depends upon the number N_i of the installed items of the i-th component and its specific cost c_i. Similarly, for all components but diesel generators, O&M costs are assumed to be proportional to N_i and the specific yearly cost m_i, accounting for the discounting factor d_y, as in (3); in the case of diesel generators, the operational charges are modelled as a function of the diesel price π^f, the fuel consumption $FC_{y,h,g}$, the number of operating hours of the units, accounting for the number of dispatched units $U_{y,h,g}$ in each time step, and their specific maintenance and replacement costs, as detailed in (4). The replacement costs RC_g of the generators are accounted for as in (5), with h_g^{life} maximum number of operating hours, whereas the ones of the battery are detailed in (6); $k_{y,h,b}$ represents the cumulative number of battery replacement and y_i^{life} is the expected lifetime of each component. Finally, the residual value RV_i of all assets is detailed in (7), as proportional to the remaining lifetime of each asset with the exception of the generator and the battery storage; $|Y|$ represents the project lifetime. The replacement charges of the generators are gradually accounted for as in (5), so they are not included in the final residual value; whereas the formulation of RV_b for the batteries is detailed in (8), as proportional to the remaining capacity of the battery; $\overline{C}_b$ and $\underline{C}_b$

represent the capacity of a battery in brand-new and aged conditions.

$$\min NPC = \sum_i (IC_i + O\&M_i + RC_i - SV_i) \tag{1}$$

$$IC_i = N_i \cdot c_i \tag{2}$$

$$O\&M_{i\setminus\{g\}} = N_i \cdot m_i \sum_y d_y \tag{3}$$

$$O\&M_g = \sum_{y,h} d_y (m_g \cdot U_{y,h,g} + \pi^f \cdot FC_{y,h,g}) \tag{4}$$

$$RC_g = \frac{c_g}{h_g^{life}} \sum_{y,h} d_y \cdot U_{y,h,g} \tag{5}$$

$$RC_b = N_b \cdot c_b \sum_{y,h} d_y (k_{y,h,b} - k_{y,h-1,b}) \tag{6}$$

$$RV_{i\setminus\{g,b\}} = d_{|Y|} \cdot N_i \cdot c_i \cdot \frac{y_i^{life} - |Y|}{y_i^{life}} \tag{7}$$

$$RV_b = d_{|Y|} \cdot c_b \frac{C^{res}_{|Y|,|H|,b} - N_b \underline{C}_b}{\overline{C}_b - \underline{C}_b} \tag{8}$$

2.2.2. Emissions

Environmental objectives have become increasingly included in planning energy projects, due to the climate-change concerns. In order to perform an accurate evaluation of the microgrid global impact, emissions have been considered in the proposed methodology in terms of LCA, i.e. accounting for construction, installation, operation and disposal of the assets. The minimization of total emission allows to evaluate solutions in line with the increasing pressure of governments for energy production with a high penetration of renewables. The mathematical formulation of CO_2 emissions is reported in (9), where $CCO2_i$ represents the emissions for the installation and replacement of the asset i and $OCO2_i$ corresponds to the CO_2 emissions due to the operation phase, which is non-null only for fuel-fired generators, as detailed in (13); e_i is the specific emission for each installed component and e_g^{op} represents the specific emission per unit of fuel consumption. $CCO2_i$ of renewable assets is detailed in (10), while its formulation for the battery and

the generator, (11) and (12), respectively, also accounts for their replacement.

$$\min CO2 = \sum_i CCO2_i + OCO2_i \tag{9}$$

$$CCO2_{i/\{g,b\}} = N_i \cdot e_i \tag{10}$$

$$CCO2_b = \left[1 + \sum_{y,h}(k_{y,h,b} - k_{y,h-1,b})\right] N_b \cdot e_b \tag{11}$$

$$CCO2_g = N_g \cdot e_g + \sum_{y,h} U_{y,h,g} \cdot \frac{e_g}{y_g^{life}} \tag{12}$$

$$OCO2_g = FC_{y,h,g} \cdot e_g^{op} \tag{13}$$

2.2.3. Land use

The local environmental impact of the microgrid is taken into account by including in the analysis the minimization of the space required for the installation of the different assets [27]. The importance of this variable for decision-makers is strictly related to the specific conditions of the area where the system needs to be installed; a case in which land occupation may become a sensitive issue is for example when the community is based in a protected area. The mathematical formulation of the land use (LU) is then considered and its model (14) is proportional to the number of installed units and their land occupation lo_i.

$$\min LU = \sum_i N_i \cdot lo_i \tag{14}$$

2.2.4. Jobs creation

Energy planning can promote local jobs, as a consequence of the assets installation and operation, which are incorporated in the proposed multi-objective method by means of a maximization problem [27–29]. The mathematical formulation of the job creation JC, detailed in (15), is a function of the jobs generated throughout the value chain of each asset (CJC_i). Moreover, the contribution related to fuel consumption for fuel-fired generators is accounted by means of a separate variable (OJC_g). Their mathematical formulation is detailed in (16)-(18), where j_i and j_i^{op} represent the specific

job creation per installation and operation of each asset.

$$\max JC = \sum_{i} CJC_i + OJC_g \tag{15}$$

$$CJC_{i/\{g\}} = N_i \cdot j_i \tag{16}$$

$$CJC_g = N_g \cdot j_g + \sum_{y,h} U^{dg}_{y,h} \cdot \frac{j_g}{y^{life}_g} \tag{17}$$

$$OJC_g = \sum_{y,h} P^{dg}_{y,h,g} \cdot j^{op}_g \tag{18}$$

2.2.5. Public lighting coverage

Finally, public lighting (PL) is considered and included in the optimization, as it is an important enabler of better living conditions, including but not limited to improved security, recreational and educational activities. Street lights are considered as priority loads: once a street light is installed, it must be supplied during the dark hours. Equation (19) maximizes the coverage of the service L^{light}, evaluated according to the needs of the community and varying in the range $1 \div 100\%$.

$$\max PL = L^{light} \tag{19}$$

2.3. Main constraints

The electric balance is guaranteed by (20), where $P^{dch}_{y,h,b}$ and $P^{ch}_{y,h,b}$ are the discharging and charging power from the battery system of type b, $\eta_{y,h,b}$ is the efficiency of the battery as function of the power rate, $P^{ren}_{y,h}$ is total power dispatched by renewable assets, $P^{dg}_{y,h,g}$ is the power produced by the fuel-fired units of type g, $D^{u}_{y,h}$ is the unmet demand, and $D_{y,h}$ and $L^{light}_{y,h}$ represent the electric demand due to load and street lighting at any year, which are defined in (21) and (22), accounting for the demand growth δ. The lighting demand is defined in (22) as the product between the proportion of lighting service to be put in place (L^{light}) and the profile pattern $L_{y,h}$ of the street lighting when all the village benefits from this service.

The unmet demand cannot be higher than the actual demand (see (23)) and it is limited by a yearly cap represented by the per-unit fraction f^u in (24). A reasonable amount of load shedding, to be defined according to local socio-economic information, is generally admitted in rural areas, as long as it enables a reduction of the electricity tariff.

The dispatched power from renewable sources ($P^{ren}_{y,h}$) is limited by the size of the number of the photovoltaic modules (N_p) and wind turbines (N_w), and their specific hourly production, $P^{pv}_{y,h,p}$ and $P^{w}_{y,h,w}$ respectively, as stated in (25). The degradation of the renewable assets is taken into account by a linear trend described with coefficients $\rho^{pv}_{y,h,p}$ and $\rho^{wt}_{y,h,w}$ for the PV plant and wind farm, respectively.

$$\sum_b \left(P^{dch}_{y,h,b} \cdot \eta_{y,h,b} - \frac{P^{ch}_{y,h,b}}{\eta_{y,h,b}} \right) + P^{ren}_{y,h} + \\ + \sum_g P^{dg}_{y,h,g} + D^{u}_{y,h} = D_{y,h} + L^{light}_{y,h} \tag{20}$$

$$D_{y,h} = D_{1,h}(1+\delta)^y \tag{21}$$

$$L^{light}_{y,h} = L^{light} \cdot L_{y,h} \tag{22}$$

$$D^{u}_{y,h} \leq D_{y,h} \tag{23}$$

$$\sum_h D^{u}_{y,h} \leq f^u \sum_h D_{y,h} \tag{24}$$

$$P^{ren}_{y,h} \leq \sum_p N_p \cdot P^{pv}_{y,h,p} \cdot \rho^{pv}_{y,h,p} + \sum_w N_w \cdot P^{wt}_{y,h,w} \cdot \rho^{wt}_{y,h,w} \tag{25}$$

Constraints (26)-(29) detail the mathematical description of the fuel-fired generators, for every technology g taken into consideration. Equation (26) describes the model of the fuel consumption $FC_{y,h,g}$ as a piece-wise linear function with respect to the number of the committed units $U_{y,h,g}$ and their total production $P^{dg}_{y,h,g}$, by technology; a and b are the corresponding parameters. The maximum and minimum power boundaries are expressed by (27) and (28), respectively, where $\overline{P}_g$ and $\underline{P}_g$ represent the maximum and minimum power limits of dispatched generators, while equation (29) guarantees that the number ($U_{y,h,g}$) of the dispatched units is no greater than the number of installed generators. $R^{dg}_{y,h,g}$ represents the upward reserve.

$$FC_{y,h,g} = a \cdot U_{y,h,g} + b \cdot P^{dg}_{y,h,g} \tag{26}$$

$$P^{dg}_{y,h,g} + R^{dg}_{y,h,g} \leq \overline{P}_g \cdot U_{y,h,g} \tag{27}$$

$$P^{dg}_{y,h,g} \geq \underline{P}_g \cdot U_{y,h,g} \tag{28}$$

$$U_{y,h,g} \leq N_g \tag{29}$$

The equation block from (30) to (36) describes the model of the battery storage by technology b. While (30) depicts the energy balance in the battery, (31) and (32) detail the maximum and the minimum state of charge of the battery, DOD_b being the maximum Depth Of Discharge; $Q_{y,h,b}$ represents the energy available in the storage bank of type b in every time step of the simulation. It is worth noticing that $C^{res}_{y,h,b}$ models the total capacity of the battery, accounting for its degradation as stated in the following subsection. The power limits of the batteries are instead managed by constraints (33)-(36); N_b represents the number of batteries, each one having $\overline{C}_b$ nominal capacity, and $\overline{PQ}_b$ represents the maximum power-to-energy ratio. $w^{dch}_{y,h,b}$ is a binary variable used to guarantee that charging and discharging cannot occur in the same time step and M is a large constant value. $R^{sb}_{y,h,b}$ of equation (32) represents the total reserve power of the storage system.

$$Q_{y,h,b} = Q_{y,h-1,b} + (P^{ch}_{y,h,b} - P^{dch}_{y,h,b})\Delta h \tag{30}$$

$$Q_{y,h,b} \leq C^{res}_{y,h,b} \tag{31}$$

$$Q_{y,h,b} \geq N_b \cdot \overline{C}_b(1 - DOD_b) + R^{sb}_{y,h,b} \cdot \Delta h \tag{32}$$

$$P^{dch}_{y,h,b} + R^{sb}_{y,h,b} \leq C^{res}_{y,h,b} \cdot \overline{PQ}_b \tag{33}$$

$$P^{ch}_{y,h,b} \leq C^{res}_{y,h,b} \cdot \overline{PQ}_b \tag{34}$$

$$P^{dch}_{y,h,b} \leq w^{dch}_{y,h,b} \cdot M \tag{35}$$

$$P^{ch}_{y,h,b} \leq (1 - w^{dch}_{y,h,b}) \cdot M \tag{36}$$

Finally, the reserve requirements are detailed by (37) and (38). Equation (37) expresses the total reserve requirements $R_{y,h}$ as a function of the demand and the renewable sources, which shall be covered by the reserve bands of the batteries and fuel-fired generators, modelled by $R^{dg}_{y,h,g}$ and $R^{sb}_{y,h,b}$, respectively. The coefficients γ_d, γ_{pv} and γ_{wt}, represent the contribution to reserve requirements of load, photovoltaic production and wind generation, respectively, in every time step of the simulation.

$$R_{y,h} = \gamma_d \cdot D_{y,h} + \gamma_{pv} \sum_p N_p \cdot p^{pv}_{y,h,p} + \gamma_{wt} \sum_w N_w \cdot p^{wt}_{y,h,w} \tag{37}$$

$$R_{y,h} \leq \sum_g R^{dg}_{y,h,g} + \sum_b R^{sb}_{y,h,b} \cdot \eta_{h,y,b} \tag{38}$$

2.4. The model of the battery efficiency

The efficiency $\hat{\eta}_{y,h,b}$ of the battery system is calculated as function of the power-to-energy ratio [16, 17]: the higher the power flow from the battery,

the lower the efficiency. In particular, a step-wise function ($\hat{\eta}_b(PQ_{y,h,b})$) dependent upon the power ratio $PQ_{y,h,b}$, computed as in (39), is used to model the efficiency in every time step, as detailed in (40).

$$PQ_{y,h,b} = \frac{P^{ch}_{y,h,b} + P^{dch}_{y,h,b}}{N_b \cdot \overline{C}_b} \tag{39}$$

$$\hat{\eta}_{y,h,b} = \eta_b(PQ_{y,h,b}) \tag{40}$$

It is worth noticing that the direct implementation of the efficiency model of $\hat{\eta}_{y,h,b}$ in the previous section, which means setting $\hat{\eta}_{y,h,b} = \eta_{y,h,b}$, would make the problem significantly non-linear and hard to solve. For this reason, the iterative approach described in the following section is used.

2.5. The degradation of the battery system

The storage system is critical for most off-grid applications and its degradation can affect the profitability of the system, thus the battery model accounts for the degradation as in [17]. In particular, the residual capacity $\hat{C}^{res}_{y,h,b}$ of the battery defined in (42) for every type b is calculated as a function of the energy throughput $Q_{y,h,b}$, detailed in (41). The formulation accounts for the variable degradation rate depending on charging and discharging power-to-energy ratio, modelled by the coefficient on maximum number of cycles $n^{cyc}_{y,h,b}(PQ_{y,h,b})$. When the useful battery capacity falls below a given threshold ($\underline{\alpha}_b$), the battery is replaced, the available capacity is restored to the initial value and the counter $k_{y,h,b}$ stating the number of replacements is updated.

$$Q^{thr}_{h,b} = Q^{thr}_{h-1,b} + (P^{ch}_{h,b} + P^{dch}_{h,b})\Delta h \tag{41}$$

$$\hat{C}^{res}_{y,h,b} = \begin{cases} \hat{C}^{res}_{y,h-1,b} - \dfrac{(1-\underline{\alpha}_b)\left(Q^{thr}_{y,h,b} - Q^{thr}_{y,h-1,b}\right)}{2n^{cyc}_{y,h,b}(PQ_{y,h,b})DOD_b} & \dfrac{\hat{C}^{res}_{y,h-1,b}}{N_b\overline{C}_b} \geq 1-\underline{\alpha}_b \\ N_b\overline{C}_b & \dfrac{\hat{C}^{res}_{y,h-1,b}}{N_b\overline{C}_b} < 1-\underline{\alpha}_b \end{cases} \tag{42}$$

Similarly to the variable efficiency model, setting $\hat{C}^{res}_{y,h,b} = C^{res}_{y,h,b}$ would mean to include in the main model a non-linear battery degradation model. In the following subsection a simplified iterative approach is proposed to overcome this complexity.

2.6. The iterative model

The model discussed in Sections 2.4 and 2.5 is significantly non-linear. Therefore, in this study, based on the iterative approach discussed in [17], the non-linearities of variables $C^{res}_{y,h,b}$ and $\eta_{y,h,b}$ are calculated externally to the MILP with off-line computations, as depicted in Figure 2. To do so, the two variables are modelled as in (43) and (44), where parameters $\alpha_{y,h,b}|_{it}$ and $\beta_{y,h,b}|_{it}$ vary in the range $1 \div 100\%$ and represent the hourly available storage capacity and efficiency with respect to their nominal values $N_b \cdot \overline{C}_b$ and $\overline{\eta}_b$. $\alpha_{y,h,b}|_{it}$ and $\beta_{y,h,b}|_{it}$ are updated in every iteration it to account for such non-linear phenomena in a MILP model, using a computationally efficient procedure.

$$C^{res}_{y,h,b} = \alpha_{y,h,b}|_{it} \cdot N_b \cdot \overline{C}_b \tag{43}$$

$$\eta_{y,h,b} = \beta_{y,h,b}|_{it} \cdot \overline{\eta}_b \tag{44}$$

As shown in Figure 2, after each MILP iteration, the values of $\alpha_{y,h,b}|_{it+1}$ and $\beta_{y,h,b}|_{it+1}$ for the following iteration $(it+1)$ are computed as in (45) and (46), based on the values of $\hat{C}^{res}_{y,h,b}$ and $\hat{\eta}_{y,h,b}$ calculated downstream of the planning procedure of the current iteration it. The algorithm stops when the relative changes of the parameters over consecutive simulations fall below a given threshold; more details of the procedure are discussed in [17].

$$\alpha_{y,h,b}|_{it+1} = \frac{\hat{C}^{res}_{y,h,b}\Big|_{it}}{N_b \cdot \overline{C}_b} \tag{45}$$

$$\beta_{y,h,b}|_{it+1} = \frac{\hat{\eta}_{y,h,b}|_{it}}{\overline{\eta}_b} \tag{46}$$

3. Multi-objective optimization

A generic multi-objective optimization can be expressed as follows:

$$\begin{aligned} &\max f(\mathbf{x}) = [f_1(\mathbf{x}), f_2(\mathbf{x}), ..., f_p(\mathbf{x})]^T \\ &s.t. y_i(\mathbf{x}) \leq 0 \qquad i \in 1...m \\ &\quad h_l(\mathbf{x}) = 0 \qquad l \in 1...q \\ &\quad \mathbf{x} = [x_1, x_2, ..., x_n]^T \end{aligned} \tag{47}$$

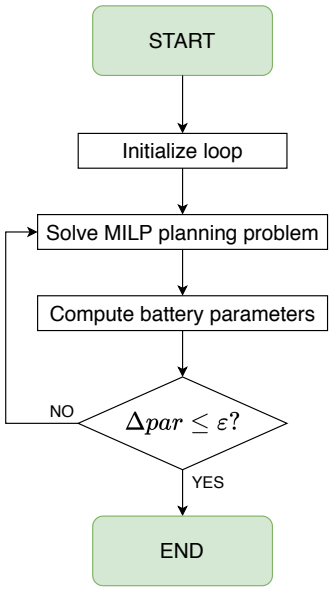

Figure 2: The optimization algorithm [17].

where $f(\mathbf{x})$ is the p-dimensional vector of objective functions, defined by the n-dimensional vector of decision variables $\mathbf{x}$. The problem is subject to m inequality constraints and q equality constraints. For the sake of simplicity, we describe a problem where all objective functions are maximized, but the same considerations follow also for minimization or mixed maximization/minimization problems.

The goal of multi-objective optimizations is to find the solutions as close as possible to the Pareto frontier, which is composed by the set of so-called non-dominated points, i.e. solutions in which the performance of one objective function cannot be improved without worsening at least one other objective function [40, 48].

3.1. ε-constraint method

3.1.1. Classic formulation

One of the most common and efficient techniques for solving multi-objective problems with MILP optimization is the ε-constraint method [40], where the multi-objective problem is transformed into several single-objective optimization problems, as shown in (48), by using an iterative approach. In partic-

ular, in every iteration, only the first objective function is optimized, while the optimization of the others is incorporated as constraints: every objective function $f_k(\mathbf{x})$ but the first, is constrained to be higher than a constant value e_k^{it}, which is modified in every iteration it. By varying e_k^{it} between the maximum ($\overline{e}_k$) and minimum ($\underline{e}_k$) values of each objective function, calculated beforehand, the procedure is able to calculate an approximation of the Pareto frontier [40, 48]. It is worth noticing that the maximum and minimum values of e_k^{it} are calculated by solving p optimization problems corresponding to the maximization of each $f_k(\mathbf{x})$ one at a time, disregarding the other $f_{j\neq k}(\mathbf{x})$. The results are stored in the payoff table and upper and lower bounds for each objective function are identified.

$$\begin{aligned} &\max f_1(\mathbf{x}) \\ &s.t. f_2(\mathbf{x}) \geq e_2^{it} \\ &\quad f_3(\mathbf{x}) \geq e_3^{it} \\ &\quad ... \\ &\quad f_p(\mathbf{x}) \geq e_p^{it} \\ &\quad y_i(\mathbf{x}) \leq 0 \qquad i \in 1...m \\ &\quad h_l(\mathbf{x}) = 0 \qquad l \in 1...q \\ &\quad \mathbf{x} = [x_1, x_2, ..., x_n]^T \end{aligned} \tag{48}$$

As typically done, the parameters e_k^{it} span between $\overline{e}_k$ and $\underline{e}_k$ with a uniform distribution divided into g_k intervals and $(g_k + 1)$ points, with a resolution of $step_k = \frac{r_k}{g_k}$, where $r_k = \overline{e}_k - \underline{e}_k$ represents the range of variation of the objective function k. With this formulation, each optimization (48) is carried out on a specific subspace of the search space, which can be described as a p-dimensional matrix of points. For every iteration it, the values of parameters e_k^{it} can be calculated as $e_k = \underline{e}_k + i_k^{it} \cdot step_k$, where $i_k^{it} \in \{1, ..., g_k + 1\}$ is the integer value representing the current position in the grid.

The total number of points in the grid is $(g_2+1)\cdot(g_3+1)\cdot...\cdot(g_k+1)$, which leads to an exponential behaviour. Therefore, the computational complexity can be very challenging as the number of objective functions increases.

When the optimization of a grid point leads to a better performance with respect to the thresholds forced by the vector $\mathbf{e}$, all the optimizations with intermediate positions of $\mathbf{e}$ will be characterized by very similar results (exactly the same Pareto point in case of null optimality gap). Moreover, the information from initial optimizations used to identify the limits of the e_k^{it}

parameters is not used in the main iterative algorithm (48). This means that the standard ε-constraint method can lead to a large number of redundant optimizations that significantly increases the computational requirements.

3.1.2. AUGMECON2

The augmented ε-constraint method, a significant improvement of the ε-constraint method, was proposed by Mavrotas and named AUGMECON2 in its most recent development [7, 8]. Conversely to the classic approach in which the extreme values ($\overline{e}_k$ and $\underline{e}_k$) of the objective functions are calculated by simply optimizing one objective function at a time, AUGMECON2 makes use of lexicographic optimization for every objective function: problem (49), with J initially empty, is sequentially solved over the set of p objective functions by adding at the end of every iteration the constraint $(f_j(\mathbf{x}) \geq \hat{f}_j)$ updating J. This guarantees that the forthcoming optimization does not deteriorate the optimality of the previous objective functions, as $\hat{f}_j$ represents the best value of objective function j. This limits the search space only to Pareto optimal solutions. The procedure is solved p times, covering the entire set of objective functions, for a total of p^2 optimization problems to solve.

$$\begin{aligned} \hat{f}_k = & \max \ f_k(\mathbf{x}) \\ & s.t. f_j(\mathbf{x}) \geq \hat{f}_j \qquad j \in J \\ & y_i(\mathbf{x}) \leq 0 \qquad i \in 1...m \\ & h_l(\mathbf{x}) = 0 \qquad l \in 1...q \\ & \mathbf{x} = [x_1, x_2, ..., x_n]^T \end{aligned} \tag{49}$$

Moreover, problem (48) is modified as follows, where $\mathbf{s} = [s_2, s_3, ...s_p]^T$ is the vector of slack variables that introduce a penalty when objective functions do not correspond to their desired values e_k^{it}, eps is an adequately small

number:

$$\begin{aligned}
&\max(f_1(\mathbf{x}) + eps \cdot (s_2/r_2 + 10^{-1} \cdot s_3/r_3 + \\
&\quad + ... + 10^{-(p-2)} \cdot s_p/r_p)) \\
&s.t. f_2(\mathbf{x}) - s_2 = e_2^{it} \\
&\quad f_3(\mathbf{x}) - s_3 = e_3^{it} \\
&\quad ... \\
&\quad f_p(\mathbf{x}) - s_p = e_p^{it} \\
&\quad y_i(\mathbf{x}) \leq 0 \quad i \in 1...m \\
&\quad h_l(\mathbf{x}) = 0 \quad l \in 1...q \\
&\quad \mathbf{x} = [x_1, x_2, ..., x_n]^T
\end{aligned} \tag{50}$$

This configuration of the objective function allows avoiding weakly efficient points. Moreover, to partially reduce the above stated problem of the presence of redundant points, the ratio $s_2/step_2$ is exploited to bypass the redundant points of the innermost loop only, i.e. the loop on e_2. This is a significant limitation that would lead to a considerable increase in computational requirements when more than two objective functions are used.

3.2. The novel A-AUGMECON2

Even if AUGMECON2 is one of the most efficient multi-objective methodologies, the computational burden is still a big issue, especially for computationally intensive algorithms like the one detailed in Section 2; hence inefficiencies, such as redundant simulations, shall be preemptively removed.

The number of grid points to be analysed grows exponentially with the number of objective functions and with the desired density of the Pareto curve. Moreover, the curve tends to present conglomerates of almost identical points, not of interest for the decision maker. This is due to the fact that the very valuable information contained in the slack variables is only used by AUGMECON2 to bypass redundant points on the innermost loop.

A-AUGMECON2, whose source code is publicly available (see Appendix), tackles the problem by limiting the calculation of points only to those whose embedded information is worth to be included in the curve, thus minimizing the computational time.

Two main actions allow limiting the number of points computed:

1. Redundant simulations are preemptively recognized and not performed for all objective functions: slack variables $\mathbf{s}$ are used to identify the redundant grid points.
2. Redundant simulations corresponding to the points obtained to draw the extreme points ($\overline{e}_k$ and $\underline{e}_k$) of the search space are not repeated.

3.2.1. Computation of the payoff table

The priority order adopted in AUGMECON2 for the lexicographic optimization of the payoff table, does not reflect the optimization order used in the iterative algorithm for the creation of the Pareto frontier; hence, payoff table points cannot be used to remove simulations in the following step. Conversely, the priority among the objective functions is designed in A-AUGMECON2 to reflect the procedure of the iterative loop and avoid redundant optimizations.

To achieve this, the priority order of the objective functions in the lexicographic optimization needs to be modified in such a way that, instead of simply following the order in which the objective functions are listed in the set as in AUGMECON2, once the k-th objective function with the highest priority has been optimized, the second highest priority is attributed to $f_1(\mathbf{x})$; after these two rounds, the rest of the objective functions can be sequentially optimized following the order in which they are listed in the set. As in AUGMECON2, constraints are added at the end of every iteration to prevent the optimizer from worsening the optimality of the previous solutions. The mathematical description is detailed in Algorithm 1.

For the sake of clarity, Table 1 compares the order followed in the lexicographic optimization for the computation of the payoff table in AUGMECON2 and A-AUGMECON2, in the case of p=3 objective functions. While the former simply follows the order in which the objective functions are listed in the pertaining set, the latter employs Algorithm 1 to always have f_1 as second highest priority (besides the first optimization, in which it is optimized as first). The A-AUGMECON2 approach allows to obtain a payoff table that contains points belonging to the Pareto curve; those points can be automatically included in the final results, thus avoiding their re-optimization in the iterative procedure to build the Pareto frontier.

Moreover, the hard constraints on the objective functions introduced by the sequential optimizations (see line 9 of Algorithm 1) are turned into soft constraints, i.e. penalties are associated to the differences from the desired values $\hat{f}_j$, in order to avoid infeasibilities that may occur in case of non-null

Algorithm 1 Defining the bounds with the new priority order for lexicographic optimization.

for $k \in \{1, 2, ..., p\}$ **do**
  for $kk \in \{1, 2, ..., p\}$ **do**
    if $kk = 1$ **then**
      Solve (49) with $f_{j=k}(\mathbf{x})$ obj. function; store solution $\hat{f}_{k,k}$
    else if $kk \leq k$ **then**
      Solve (49) with $f_{j=kk-1}(\mathbf{x})$ obj. function; store solution $\hat{f}_{k,kk-1}$
    else
      Solve (49) with $f_{j=kk}$ obj. function; store solution $\hat{f}_{k,kk}$
    Add constraint $f_j(\mathbf{x}) \geq \hat{f}_j$
  Save final solution into payoff table
Calculate bounds: $\underline{e}_k = \min_{\hat{k} \in \{1..p\}} \hat{f}_{\hat{k},k}$ and $\overline{e}_k = \max_{\hat{k} \in \{1..p\}} \hat{f}_{\hat{k},k}$

optimality gap.

3.2.2. Construction of Pareto frontier with online filter

The procedure to find the efficient solutions is shown in Figure 3 and described in this section.

First, the payoff table is completed and the ranges of variation r_k of objective functions $f_2(\mathbf{x}), ..., f_p(\mathbf{x})$ are divided into g_k intervals to identify the grid of $(g_2 + 1) \cdot (g_3 + 1) \cdot ... \cdot (g_k + 1)$ points, corresponding to the maximum number of iterations to be performed, as detailed in the previous section. Then, after the initialization of given indices, the main iterative loop starts.

Table 1: Priority order in lexicographic optimization for p=3, in AUGMECON2 and A-AUGMECON2.

	AUGMECON2	A-AUGMECON2
it=1	$f_1 \rightarrow f_2 \rightarrow f_3$	$f_1 \rightarrow f_2 \rightarrow f_3$
it=2	$f_2 \rightarrow f_3 \rightarrow f_1$	$f_2 \rightarrow f_1 \rightarrow f_3$
it=3	$f_3 \rightarrow f_1 \rightarrow f_2$	$f_3 \rightarrow f_1 \rightarrow f_2$

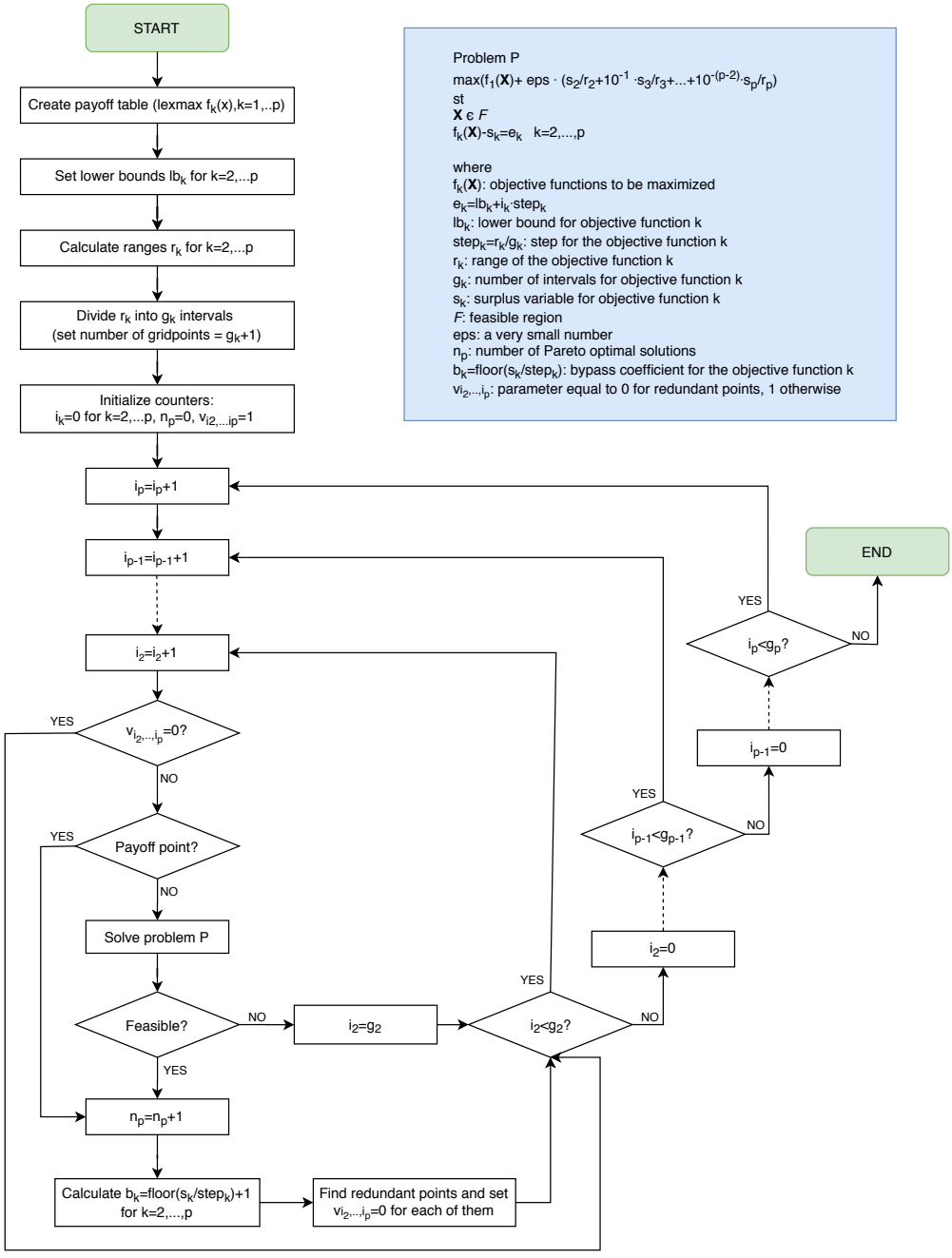

Figure 3: Flowchart of the proposed methodology.

In order to improve the computational performances and the readability of the results, an online filter skipping the redundant points is implemented in every iteration. Each point is associated with a parameter $v_{i_2,...,i_p}$, where $\mathbf{i} = [i_2, ..., i_p]^T$ is the position vector of the point in the grid. The parameter has value 1 if the point shall be analysed, 0 if it shall be skipped. At the beginning of the procedure, the vector $\mathbf{v}$ of all $v_{i_2,...,i_p}$ is initialized to analyse all points (vector of ones).

The optimization of a given iteration is performed only if the corresponding $v_{i_2,...,i_p}$ equals 1 and if the position of the point in the grid does not correspond to a point already calculated in the payoff table. If this last condition occurs, the results obtained from the lexicographic optimization to form the payoff table, as per Section 3.2.1, are directly included in the Pareto frontier, thus avoiding the repetition of its calculation.

When the current iteration corresponds to a non-redundant solution, then the optimization is performed and the outcome is collected; when a non-feasible solution is returned, points characterized by more stringent thresholds are skipped, as they are expected to provide non-feasible solutions, too.

When a feasible solution is obtained, it is stored in the repository of the Pareto curve and the result is analysed to evaluate whether some redundant simulations shall be removed from the analysis by setting the corresponding $v_{\mathbf{i}} = 0$. To do so, the bypass coefficient $b_k = floor(s_k/step_k) + 1$ is computed for $k = 2, ..., p$, where $floor(\cdot)$ returns the integer part of the number. Then, Algorithm 2 is adopted to determine all the N_{comb} combinations of $i_2, ..., i_p$ identifying the points of the grid that would produce a similar result, where $comb$ and Δi_k are parameters and $mod(\cdot)$ is a function that returns the remainder of the division. The parameter $v_{i_2,...,i_p}$ of the N_{comb} redundant points is set to zero.

Algorithm 2 Defining the positions of redundant points.

1: $b_k = floor(s_k/step_k) + 1$, $k \in 1, 2, ..., p$
2: $N_{comb} = \prod_{k=2}^{p} b_k$
3: **for** $comb \in 0, ..., N_{comb} - 1$ **do**
4: **for** $k \in 2, ..., p$ **do**
5: $\Delta i_k = mod(comb/b_k)$
6: $comb = floor(comb/b_k)$
7: $i_k = i_k + \Delta i_k$
8: $v_{i_2,...,i_p} = 0$

Finally, the parameters $i_2, ..., i_p$ are updated to move forward in the grid. The procedure stops when the condition $i_k = g_k + 1$ holds for $k = 2, ..., p$.

For the sake of clarity, Figure 4 illustrates the procedure in presence of redundant optimizations for the case of p=3 objective functions, where $f_1(\mathbf{x})$ is optimized, while $f_2(\mathbf{x})$ and $f_3(\mathbf{x})$, both varying in the range $1 \div 4$, are turned into constraints. Point U_{it}, identified by the green square, is the grid element to be analysed. It lies in position $\mathbf{i}_U = [2, 1]$, i.e. problem (50) is subject to the constraints $(f_2(\mathbf{x}) - s_2 = 2)$ and $(f_3(\mathbf{x}) - s_3 = 1)$. As $v_{\mathbf{i}_U} = 1$, the optimization is not redundant and must be carried out. The problem corresponding to the grid point U_{it} is solved; the results, shown in Figure 4, are characterized by $s_2 = 1$ and $s_3 = 2$. Applying Algorithm 2, $v_{\mathbf{i}}$ is set to zero for $N_{comb} = 6$ points, including the current grid point and 5 redundant iterations, represented as red dots in Figure 4. Then, the grid is crossed in the direction of the blue arrow, according to the order in which objective functions are listed in the related set, i.e. along f_2 first, then along f_3. Therefore, the following point to be analysed is U_{it+1}.

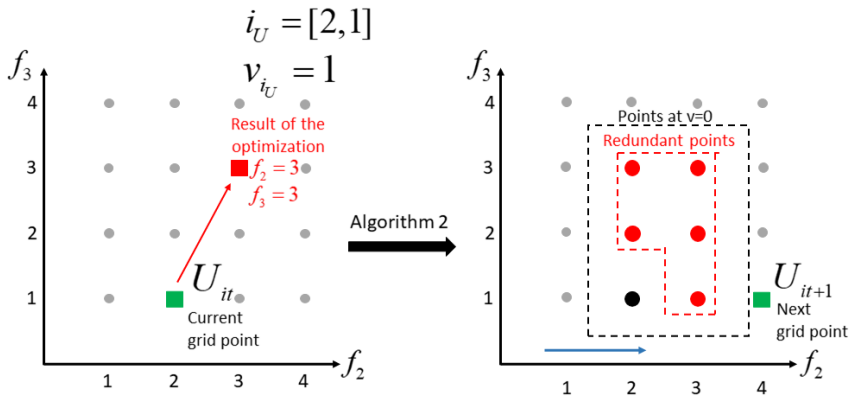

Figure 4: Procedure to skip redundant optimizations in case p=3.

4. Case study

4.1. Description

The proposed methodology has been tested on the case study of the rural community of Soroti, Uganda, accounting for about 100 households and small commercial activities. Given the location and climate of the site,

a photovoltaic plant and a wind farm are possible technology candidates for the system along with lithium storage and fuel-fired generation, as shown in Figure 1.

4.2. Load and renewable production

The initial load curve, shown in Figure 5, has been estimated in [49] by means of on-field surveys and stochastic analysis. A 2% annual growth has been considered [50].

The specific renewable and wind power production per unit of asset has been estimated using the Renewable.ninja platform [51, 52].

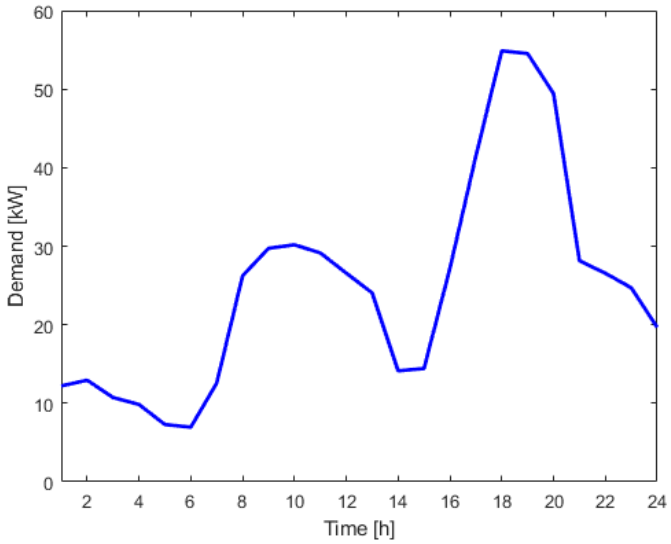

Figure 5: Initial daily load.

4.3. Input parameters

According to the proposed multi-objective approach aligned with the Sustainable Development Goals, the three sustainability dimensions, economic, environmental and social, have been taken into account. The main economic parameters of the optimization are summarized in Table 2; the data related to the environmental impact (global CO2 emissions and land use) are reported in Table 3; the information related to job creation is shown in Table 4, and the need for public lighting has been estimated based on on-field data collection [49].

Table 2: Components costs and lifetimes [11, 14, 17, 53].

	Unit size	c_i	m_i	FC_i	Lifetime
Photovoltaic panel	1 kW	1.1 $k€$	10 €/y	-	20 y
Wind turbine	10 kW	27 $k€$	810 €/y	-	20 y
Diesel generator	16 kW	11 $k€$	0.208 €/h	0.75 €/L	15,000 h
Battery	1 kWh	0.4 $k€$	10 €/y	-	15 y
Converter	1 kW	0.3 $k€$	-	-	20 y

It is worth noticing that, in order to investigate the global environmental impact of the proposed systems, the emissions have been evaluated with an LCA approach that allows a more in-depth and accurate impact analysis with respect to an evaluation limited to direct emissions alone. The assessment of the local environmental impact of the electrification project has been accounted for in terms of land use of the different components. As for batteries, their space requirements are considered negligible, as racks can present a very compact layout.

Table 3: Components LCA emissions and land use [31, 54, 55].

	Emissions	Land use
Photovoltaic panel	2472.07 $kgCO_2/kW$	7.1 m^2/kW
Wind turbine	935.57 $kgCO_2/kW$	267.7 m^2/kW
Diesel generator	192.17 $kgCO_2/kW$	2.35 $m^2/unit$
Fuel	3.15 $kgCO_2/L$	-
Battery	56.45 $kgCO_2/kWh$	-

Many studies have analysed the impact of different energy technologies on the job market in industrialized countries [56, 57], but little has been done to investigate this topic for rural communities in the Global South. A methodology has been developed in order to estimate multiplicative factors that allow the data of industrialized countries to be applied to different contexts [58]. Given the interest of this work in evaluating the local impacts in terms of job creation, only construction and installation (C&I) and operation and maintenance (O&M) are included and shown in Table 4, as the manufacturing of components for rural electrification projects is very likely to be performed abroad, not contributing to local development.

Table 4: Components job creation per phase [59].

	C&I [jobs/MW]	O&M [jobs/MW]	Fuel [jobs/GWh]
Photovoltaic panel	13.46	7.34	-
Wind turbine	3.06	4.90	-
Diesel generator	2.08	1.96	2.94

Asset degradation has been included in the analysis by considering a 1% annual decay of PV panel [18], a 0.53% annual deterioration of wind turbines [19], and a non-linear power-dependent degradation of batteries [60–62].

4.4. Test procedure

The multi-objective problem described in Section 2 has been modelled in GAMS 24.0.2 and solved with CPLEX, using A-AUGMECON2 method described in Section 3.2. The comparison with the standard AUGMECON2 algorithm is also proposed.

The simulations have been run on a 6-core 3.20GHz Intel Core i7 computer with 16GB RAM. A tolerance of 0.5% has been set on thresholds $\mathbf{e}$, $g_k = 6$ for $k \in \{2, ..., p\}$; hence, a grid of $\prod_{k=2}^{p}(g_k + 1) = 2401$ points is analysed. Each optimization is bound by a time limit of 30 minutes and the time frame under study is 10 years, described by means of one representative day per month.

5. Results

The proposed multi-objective optimization provides a significant contribution in terms of both methodological improvement and holistic analysis of rural electrification projects. These aspects are analysed in the following subsections.

5.1. Validation of the online Pareto pruning

Table 5 confirms that the novel methodology described in Section 3.2 allows a considerable reduction of the computational burden by skipping many redundant computations, while keeping the same quality of information about the Pareto curve. In particular, as highlighted in Table 5, the total number of points in the curve is reduced by 42% with respect to the

AUGMECON2 method, and the total time employed by A-AUGMECON2 is 48% lower. Hence, the tractability of the problem is highly improved.

Table 5: Computational performances with and without online Pareto pruning.

	Points	Computation time
AUGMECON2	240	95 h
A-AUGMECON2	139	49 h

In terms of Pareto frontier, the curve obtained with AUGMECON2 (Figure 6a) has more than four times the number of points than with the proposed A-AUGMECON2 (Figure 6b), but actually it does not enrich the portfolio of solutions; on the contrary, it hinders the readability of the results, as many points overlap without providing further information, resulting in a more difficult decision making process. Hence, the presence of the online filter does not undermine the accuracy of the results; on the contrary, it enables a more efficient analysis of the curve. Moreover, it is worth noticing that, given the limit on the duration of each optimization, AUGMECON2 was not able to identify the extreme of the curve corresponding to maximum job creation, while the proposed methodology automatically included this point without additional computations, being it in the payoff table. Therefore, Figure 6b provides a more comprehensive view of the possible solutions, even more efficiently and faster than the standard AUGMECON2.

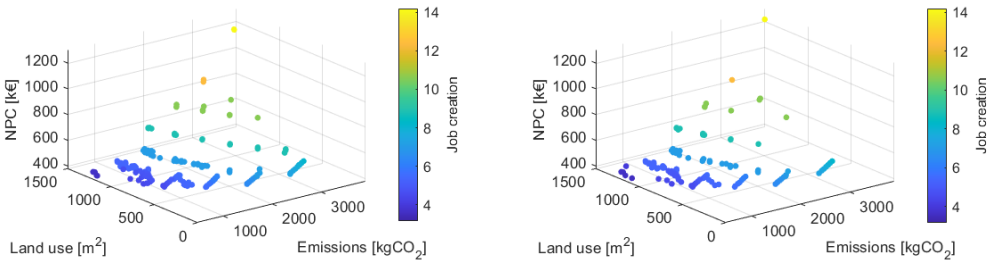

Figure 6: Optimization results using AUGMECON2 (a) and A-AUGMECON2 with online filter (b).

5.2. Discussion on numerical results

The algorithm deals with conflicting objectives and the search space is delimited by the points identified in the payoff table, in which the best performance of each objective function is evaluated as per Section 3.2.1.

As highlighted in Figure 7, the minimum NPC point is characterized by performances very similar to those of the points with minimum emissions and maximum supply of the public lighting service. This means that the three objective functions can perform very well without substantially compromising the other two. In fact, public lighting has a limited effect in terms of the other objective functions. Moreover, the economic target almost meets the environmental one because of the affordability of renewable sources. On the other hand, job creation and land use show quite poor performances in all the three points. These solutions provide for the installation of a diesel generator, about 160 kW of solar panels and more than 460 kWh of batteries.

Interestingly, it is worth noticing that the LCA approach for emissions accounting leads to a generating portfolio of the point at minimum emissions that is not entirely based on renewable sources: the diesel generator is occasionally employed at the end of the project, when the load is higher and the performances of PV panels are poorer. This is because the installation of an additional quantity of panels sufficient to cover the load for the entire duration of the project, net of the degradation phenomena, would cause a greater quantity of life-cycle emissions than those associated with the installation and occasional use of a diesel generator, providing about 2% of the total energy. This result highlights the importance of an LCA impact assessment (from cradle to grave), because limiting the analysis to direct emissions could lead to distorted and incorrect considerations.

If land use had the highest priority for the decision maker, it could be drastically reduced by installing 2 diesel generators and about 121 kWh of batteries, providing an equivalent of more than 7 full-time jobs. However, it would come with very high life-cycle emissions and a considerable increase of the NPC with respect to the least-cost option.

Finally, the maximization of jobs leads to the installation of all the available units and, consequently, to a significant oversizing. Hence, it is associated with the highest costs, emissions and land use, and the total public lighting demand can be easily satisfied. This is the only case in which wind turbines are installed.

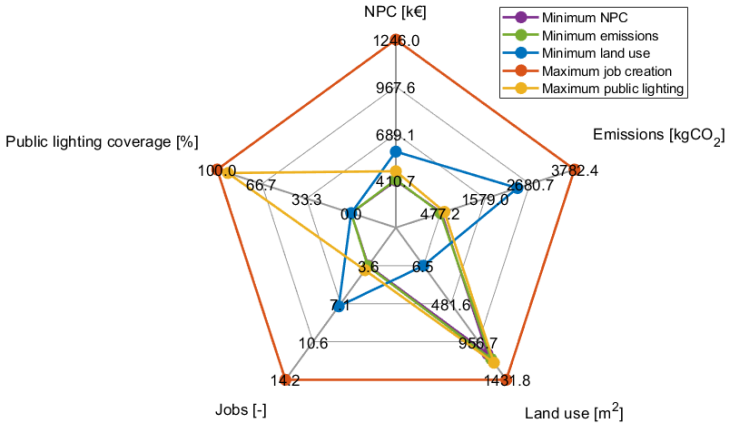

Figure 7: Payoff table points.

5.3. Narrowing down possible solutions

The output of the procedure, shown in Figure 6b, provides a comprehensive view of the problem and enables the decision maker to analyse the mutual relationships of the various objective functions. Despite the filter, which removes redundancies and improves the readability of the results, some considerations can be made to further reduce the portfolio of available options and ease the decision making process, starting from the analysis of Figures 6b and 7 and from the considerations in Section 5.2. In particular, the points of the grid with high thresholds on jobs creation (> 8) can be excluded from the analysis, as they correspond to oversized microgrids. Moreover, given the very limited influence of public lighting on the total cost of the system, it is sensible to guarantee a high share of the service, in light of the extremely positive impact it has on the well-being of the community. Therefore, only points with $PL > 90\%$ are taken into consideration. This allows to narrow the options down to the 15 points shown in Figure 8.

Figure 8a highlights that higher emissions are associated with higher costs and more people employed in the plant. In fact, the higher the reliance on diesel generators, the greater the emissions and the workforce needed to manage the supply of fuel in the system.

As previously underlined, the lowest land occupation is achieved with the installation of diesel generators, supported by batteries, which produces a rather high demand for labour. When PV panels are installed, they make up

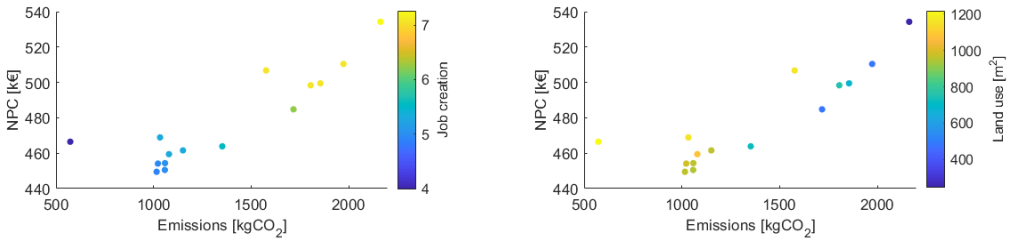

Figure 8: Cost and jobs variations depending on LCA emissions (a) and land use (b).

the prominent contribution to land take, considering that wind turbines are not installed because their limited energy production makes them inefficient in terms of both cost and land use. Figure 8b makes it possible to identify the presence of two trends: an upper curve characterized by a large land use (yellow-orange dots), and a lower one (cyan-blue dots) with lower land use needs. When comparing points of the two curves with similar NPC, it turns out that the upper curve comes with lower emissions and a related higher renewable penetration. Moreover, in case of fairly homogeneous points in terms of land use (having similar colour in Figure 8b), which also means similar PV capacity, the different capacities of the battery system and diesel generators, and therefore a different operation of the assets, highly influence the other objective functions. In particular, the operating costs of diesel generators significantly affect NPC and emissions.

5.4. Decision making process

The peculiarity of the Pareto curve obtained from multi-objective optimization is that it preserves the complexity of the problem under analysis and allows the decision maker to have a full picture of the possible solutions and of their outcomes in different scopes.

Several works adopt procedures that lead to the selection of one single point of the curve by means of mathematical methods [46, 47]. In the authors' opinion, the selection of the optimal microgrid for the purpose of rural electrification has so many impacts on the community, that it is preferable that the decision maker is able to evaluate among a reasonable number of options and to select the most appropriate according to site-specific characteristics.

Among the various qualitative criteria that can facilitate the final evaluation based on the specificities of the community are: the willingness to pay

for energy; the social acceptability of the different technologies; the compatibility with future expansion of the plant; the resilience of the system, related to the availability of components and to the ease of maintenance and training of specialized personnel [30, 31, 33].

6. Conclusions

This paper successfully proposes a multi-objective planning method for off-grid microgrids able to optimize socio-economic, security and environmental concerns in a long-term perspective, accounting for detailed multi-year simulations of the system operation and assets degradation. In order to efficiently solve the corresponding non-linear multi-objective problem, the novel A-AUGMECON2 algorithm has been developed and its results proved to improve the convergence characteristics of the standard AUGMECON2, thanks to the novel Pareto pruning method that avoids repeating redundant optimizations. Each A-AUGMECON2 optimization is integrated with an iterative approach that allows to efficiently deal with the non-linear problem by solving a number of MILP subproblems, where parameters are updated till convergence.

The results of this paper demonstrate that increasing the reliance on fuel-fired generators can improve the direct local jobs, as a consequence of the installation, maintenance and operation of the assets, and limit the land use. However, this objective is conflicting to life-cycle economic cost and global environmental impact; thus a compromise is required. Interestingly, the optimal design considering economics only leads to very good performances in terms of carbon emissions, as renewable energy sources supported by batteries can provide a reliable service at low cost. Moreover, the provision of public lighting service has a very limited impact on the generating portfolio but it has a significant impact on the well-being of the community; therefore, it is reasonable to guarantee the provision of this service when planning rural electrification projects.

The Pareto frontier obtained using the A-AUGMECON2 is equivalent to the one obtained by the standard AUGMECON2, but the computational requirements are more than halved with respect to the latter.

The corresponding Pareto frontier can guide developers and policy makers in better understanding the trade-off between multiple impacts for rural microgrids, accounting for detailed non-linear models of the assets degradation and the system operation. Moreover, A-AUGMECON2 method has

proved to effectively solve multi-objective problems and can be easily applied to other energy fields and system configurations.

Appendix A. Source code

The source code is publicly available on the GitHub platform at the following link: https://github.com/marinapet/multi-objective.

References

[1] UN Economic and Social Council, Progress towards the Sustainable Development Goals, Report of the Secretary-General (2020) 1–23.
URL https://sustainabledevelopment.un.org/content/documents/26158Final_SG_SDG_Progress_Report_14052020.pdf

[2] F. Riva, H. Ahlborg, E. Hartvigsson, S. Pachauri, E. Colombo, Electricity access and rural development: Review of complex socio-economic dynamics and causal diagrams for more appropriate energy modelling, Energy for Sustainable Development 43 (2018) 203–223. doi:10.1016/j.esd.2018.02.003.
URL https://doi.org/10.1016/j.esd.2018.02.003

[3] M.-J. Kurdziel, D. Thomas, The role of renewable energy mini-grids in Kenya's electricity sector Evidence of a cost-competitive option for rural electrification and sustainable development, Tech. Rep. November (2019).
URL https://newclimate.org/wp-content/uploads/2019/11/The-role-of-renewable-energy-mini-grids-in-Kenya's-electricity-sector.pdf

[4] F. Riva, A. Tognollo, F. Gardumi, E. Colombo, Long-term energy planning and demand forecast in remote areas of developing countries: Classification of case studies and insights from a modelling perspective, Energy Strategy Reviews 20 (2018) 71–89. doi:10.1016/j.esr.2018.02.006.
URL https://doi.org/10.1016/j.esr.2018.02.006

[5] T. R. Albrecht, A. Crootof, C. A. Scott, The Water-Energy-Food Nexus: A systematic review of methods for nexus assessment, Environmental Research Letters 13 (4) (2018). doi:10.1088/1748-9326/aaa9c6.

[6] IEA, World Energy Outlook 2020, Tech. rep. (2020).
URL https://www.iea.org/reports/world-energy-outlook-2020

[7] G. Mavrotas, Effective implementation of the ϵ-constraint method in Multi-Objective Mathematical Programming problems, Applied Mathematics and Computation 213 (2) (2009) 455–465. doi:10.1016/j.amc.2009.03.037.
URL http://dx.doi.org/10.1016/j.amc.2009.03.037

[8] G. Mavrotas, K. Florios, An improved version of the augmented s-constraint method (AUGMECON2) for finding the exact pareto set in multi-objective integer programming problems, Applied Mathematics and Computation 219 (18) (2013) 9652–9669. doi:10.1016/j.amc.2013.03.002.

[9] G. G. Moshi, C. Bovo, A. Berizzi, L. Taccari, Optimization of integrated design and operation of microgrids under uncertainty, 19th Power Systems Computation Conference, PSCC 2016 (2016). doi:10.1109/PSCC.2016.7540870.

[10] B. Li, R. Roche, A. Miraoui, Microgrid sizing with combined evolutionary algorithm and MILP unit commitment, Applied Energy 188 (2017) 547–562. doi:10.1016/j.apenergy.2016.12.038.
URL http://dx.doi.org/10.1016/j.apenergy.2016.12.038

[11] L. Moretti, M. Astolfi, C. Vergara, E. Macchi, J. I. Pérez-Arriaga, G. Manzolini, A design and dispatch optimization algorithm based on mixed integer linear programming for rural electrification, Applied Energy 233-234 (2019) 1104–1121. doi:10.1016/j.apenergy.2018.09.194.
URL https://doi.org/10.1016/j.apenergy.2018.09.194

[12] F. Riva, F. Gardumi, A. Tognollo, E. Colombo, Soft-linking energy demand and optimisation models for local long-term electricity planning: An application to rural India, Energy 166 (2019) 32–46. doi:10.1016/j.energy.2018.10.067.
URL https://doi.org/10.1016/j.energy.2018.10.067

[13] C. Brivio, M. Moncecchi, S. Mandelli, M. Merlo, A novel software package for the robust design of off-grid power systems, Journal of Cleaner

Production 166 (2017) 668–679. doi:10.1016/j.jclepro.2017.08.069.
URL http://dx.doi.org/10.1016/j.jclepro.2017.08.069

[14] D. R. Prathapaneni, K. P. Detroja, An integrated framework for optimal planning and operation schedule of microgrid under uncertainty, Sustainable Energy, Grids and Networks 19 (2019) 100232. doi:10.1016/j.segan.2019.100232.
URL https://doi.org/10.1016/j.segan.2019.100232

[15] Z. K. Pecenak, M. Stadler, K. Fahy, Efficient multi-year economic energy planning in microgrids, Applied Energy 255 (April 2019) (2019) 113771. doi:10.1016/j.apenergy.2019.113771.
URL https://doi.org/10.1016/j.apenergy.2019.113771

[16] A. Rossi, M. Stabile, C. Puglisi, D. Falabretti, M. Merlo, Evaluation of the energy storage systems impact on the Italian ancillary market, Sustainable Energy, Grids and Networks 17 (2019) 100178. doi:10.1016/j.segan.2018.11.004.
URL https://doi.org/10.1016/j.segan.2018.11.004

[17] M. Petrelli, D. Fioriti, A. Berizzi, D. Poli, Multi-year planning of a rural microgrid considering storage degradation, IEEE Transactions on Power Systems 36 (2) (2021) 1459–1469. doi:10.1109/tpwrs.2020.3020219.

[18] A. Azizi, P. O. Logerais, A. Omeiri, A. Amiar, A. Charki, O. Riou, F. Delaleux, J. F. Durastanti, Impact of the aging of a photovoltaic module on the performance of a grid-connected system, Solar Energy 174 (August) (2018) 445–454. doi:10.1016/j.solener.2018.09.022.

[19] S. D. Hamilton, D. Millstein, M. Bolinger, R. Wiser, S. Jeong, How Does Wind Project Performance Change with Age in the United States?, Joule 4 (5) (2020) 1004–1020. doi:10.1016/j.joule.2020.04.005.
URL https://doi.org/10.1016/j.joule.2020.04.005

[20] N. E. Koltsaklis, M. Giannakakis, M. C. Georgiadis, Optimal energy planning and scheduling of microgrids, Chemical Engineering Research and Design 131 (2018) 318–332. doi:10.1016/j.cherd.2017.07.030.
URL http://dx.doi.org/10.1016/j.cherd.2017.07.030

[21] J. Zhang, K. J. Li, M. Wang, W. J. Lee, H. Gao, A bi-level program for the planning of an islanded microgrid including CAES, IEEE Industry Application Society - 51st Annual Meeting, IAS 2015, Conference Record (2015) 1–8doi:10.1109/IAS.2015.7356783.
URL http://dx.doi.org/10.1109/IAS.2015.7356783

[22] B. Zhao, X. Zhang, P. Li, K. Wang, M. Xue, C. Wang, Optimal sizing, operating strategy and operational experience of a stand-alone microgrid on Dongfushan Island, Applied Energy 113 (2014) 1656–1666. doi:10.1016/j.apenergy.2013.09.015.
URL http://dx.doi.org/10.1016/j.apenergy.2013.09.015

[23] S. Mashayekh, M. Stadler, G. Cardoso, M. Heleno, A mixed integer linear programming approach for optimal DER portfolio, sizing, and placement in multi-energy microgrids, Applied Energy 187 (2017) 154–168. doi:10.1016/j.apenergy.2016.11.020.
URL http://dx.doi.org/10.1016/j.apenergy.2016.11.020

[24] F. K. Abo-Elyousr, A. Elnozahy, Bi-objective economic feasibility of hybrid micro-grid systems with multiple fuel options for islanded areas in Egypt, Renewable Energy 128 (2018) 37–56. doi:10.1016/j.renene.2018.05.066.
URL https://doi.org/10.1016/j.renene.2018.05.066

[25] M. Kharrich, O. H. Mohammed, N. Alshammari, M. Akherraz, Multi-objective optimization and the effect of the economic factors on the design of the microgrid hybrid system, Sustainable Cities and Society 65 (October 2020) (2021) 102646. doi:10.1016/j.scs.2020.102646.
URL https://doi.org/10.1016/j.scs.2020.102646

[26] M. A. Cuesta, T. Castillo-Calzadilla, C. E. Borges, A critical analysis on hybrid renewable energy modeling tools: An emerging opportunity to include social indicators to optimise systems in small communities, Renewable and Sustainable Energy Reviews 122 (2020) 109691. doi:10.1016/j.rser.2019.109691.

[27] D. Silva, T. Nakata, Multi-objective assessment of rural electrification in remote areas with poverty considerations, Energy Policy 37 (8) (2009) 3096–3108. doi:10.1016/j.enpol.2009.03.060.

[28] R. B. Hiremath, B. Kumar, P. Balachandra, N. H. Ravindranath, Bottom-up approach for decentralised energy planning: Case study of Tumkur district in India, Energy Policy 38 (2) (2010) 862–874. doi:10.1016/j.enpol.2009.10.037.

[29] R. Dufo-López, I. R. Cristóbal-Monreal, J. M. Yusta, Optimisation of PV-wind-diesel-battery stand-alone systems to minimise cost and maximise human development index and job creation, Renewable Energy 94 (2016) 280–293. doi:10.1016/j.renene.2016.03.065.

[30] F. Fuso Nerini, M. Howells, M. Bazilian, M. F. Gomez, Rural electrification options in the Brazilian Amazon. A multi-criteria analysis, Energy for Sustainable Development 20 (1) (2014) 36–48. doi:10.1016/j.esd.2014.02.005.

[31] B. Mainali, S. Silveira, Using a sustainability index to assess energy technologies for rural electrification, Renewable and Sustainable Energy Reviews 41 (2015) 1351–1365. doi:10.1016/j.rser.2014.09.018.
URL http://dx.doi.org/10.1016/j.rser.2014.09.018

[32] A. Kumar, A. R. Singh, Y. Deng, X. He, P. Kumar, R. C. Bansal, Integrated assessment of a sustainable microgrid for a remote village in hilly region, Energy Conversion and Management 180 (2019) 442–472. doi:10.1016/j.enconman.2018.10.084.
URL https://doi.org/10.1016/j.enconman.2018.10.084

[33] M. Juanpera, P. Blechinger, L. Ferrer-Martí, M. M. Hoffmann, R. Pastor, Multicriteria-based methodology for the design of rural electrification systems. A case study in Nigeria, Renewable and Sustainable Energy Reviews 133 (2020) 110243. doi:10.1016/j.rser.2020.110243.
URL https://doi.org/10.1016/j.rser.2020.110243

[34] L. Li, H. Mu, N. Li, M. Li, Economic and environmental optimization for distributed energy resource systems coupled with district energy networks, Energy 109 (2016) 947–960. doi:10.1016/j.energy.2016.05.026.
URL http://dx.doi.org/10.1016/j.energy.2016.05.026

[35] J. Martínez-Gomez, J. Peña-Lamas, M. Martín, J. M. Ponce-Ortega, A multi-objective optimization approach for the selection of working fluids

of geothermal facilities: Economic, environmental and social aspects, Journal of Environmental Management 203 (2017) 962–972. doi:10.1016/j.jenvman.2017.07.001.

[36] D. Zhang, S. Evangelisti, P. Lettieri, L. G. Papageorgiou, Optimal design of CHP-based microgrids: Multiobjective optimisation and life cycle assessment, Energy 85 (2015) 181–193. doi:10.1016/j.energy.2015.03.036.

[37] C. Cambero, T. Sowlati, Incorporating social benefits in multi-objective optimization of forest-based bioenergy and biofuel supply chains, Applied Energy 178 (2016) 721–735. doi:10.1016/j.apenergy.2016.06.079.
URL http://dx.doi.org/10.1016/j.apenergy.2016.06.079

[38] J. Zhong, T. E. Yu, C. D. Clark, B. C. English, J. A. Larson, C. L. Cheng, Effect of land use change for bioenergy production on feedstock cost and water quality, Applied Energy 210 (2018) 580–590. doi:10.1016/j.apenergy.2017.09.070.
URL https://doi.org/10.1016/j.apenergy.2017.09.070

[39] A. Berizzi, C. Bovo, M. Innorta, P. Marannino, Multiobjective optimization techniques applied to modern power systems, in: 2001 IEEE Power Engineering Society Winter Meeting, 2002, pp. 1503–1508. doi:10.1109/pesw.2001.917333.

[40] G. Chiandussi, M. Codegone, S. Ferrero, F. E. Varesio, Comparison of multi-objective optimization methodologies for engineering applications, Computers and Mathematics with Applications 63 (5) (2012) 912–942. doi:10.1016/j.camwa.2011.11.057.
URL http://dx.doi.org/10.1016/j.camwa.2011.11.057

[41] A. Jabbarzadeh, B. Fahimnia, S. Rastegar, Green and Resilient Design of Electricity Supply Chain Networks: A Multiobjective Robust Optimization Approach, IEEE Transactions on Engineering Management 66 (1) (2019) 52–72. doi:10.1109/TEM.2017.2749638.

[42] M. Wang, H. Yu, R. Jing, H. Liu, P. Chen, C. Li, Combined multi-objective optimization and robustness analysis framework for building integrated energy system under uncertainty, Energy Conversion and

Management 208 (February) (2020) 112589. doi:10.1016/j.enconman.2020.112589.
URL https://doi.org/10.1016/j.enconman.2020.112589

[43] S. Sudeng, N. Wattanapongsakorn, Post Pareto-optimal pruning algorithm for multiple objective optimization using specific extended angle dominance, Engineering Applications of Artificial Intelligence 38 (2015) 221–236. doi:10.1016/j.engappai.2014.10.020.

[44] L. Yan'Gang, Q. Zheng, A decision support system for satellite layout integrating multi-objective optimization and multi-attribute decision making, Journal of Systems Engineering and Electronics 30 (3) (2019) 535–544. doi:10.21629/JSEE.2019.03.11.

[45] M. J. Brusco, Partitioning methods for pruning the Pareto set with application to multiobjective allocation of a cross-trained workforce, Computers and Industrial Engineering 111 (2017) 29–38. doi:10.1016/j.cie.2017.06.035.
URL http://dx.doi.org/10.1016/j.cie.2017.06.035

[46] Z. Wang, G. P. Rangaiah, Application and Analysis of Methods for Selecting an Optimal Solution from the Pareto-Optimal Front obtained by Multiobjective Optimization, Industrial and Engineering Chemistry Research 56 (2) (2017) 560–574. doi:10.1021/acs.iecr.6b03453.

[47] J. M. Sanchez-Gomez, M. A. Vega-Rodríguez, C. J. Pérez, Comparison of automatic methods for reducing the Pareto front to a single solution applied to multi-document text summarization, Knowledge-Based Systems 174 (2019) 123–136. doi:10.1016/j.knosys.2019.03.002.
URL https://doi.org/10.1016/j.knosys.2019.03.002

[48] Y. Cui, Z. Geng, Q. Zhu, Y. Han, Review: Multi-objective optimization methods and application in energy saving, Energy 125 (2017) 681–704. doi:10.1016/j.energy.2017.02.174.
URL http://dx.doi.org/10.1016/j.energy.2017.02.174

[49] S. Mandelli, C. Brivio, E. Colombo, M. Merlo, A sizing methodology based on Levelized Cost of Supplied and Lost Energy for off-grid rural electrification systems, Renewable Energy 89 (2016) 475–488. doi:10.

1016/j.renene.2015.12.032.
URL http://dx.doi.org/10.1016/j.renene.2015.12.032

[50] D. P. Blechinger, E. Papadis, M. Baart, P. Telep, F. Simonsen, What Size Shall it be? A Guide to Mini-grid Sizing and Demand Forecasting, The German Climate Technology Inititiave (2016).
URL https://energypedia.info/images/0/0f/Mini-Grid_Sizing_Guidebook.pdf

[51] S. Pfenninger, I. Staffell, Long-term patterns of European PV output using 30 years of validated hourly reanalysis and satellite data, Energy 114 (2016) 1251–1265. doi:10.1016/j.energy.2016.08.060.
URL http://dx.doi.org/10.1016/j.energy.2016.08.060

[52] I. Staffell, S. Pfenninger, Using bias-corrected reanalysis to simulate current and future wind power output, Energy 114 (2016) 1224–1239. doi:10.1016/j.energy.2016.08.068.
URL http://dx.doi.org/10.1016/j.energy.2016.08.068

[53] A. Kamjoo, A. Maheri, A. M. Dizqah, G. A. Putrus, Multi-objective design under uncertainties of hybrid renewable energy system using NSGA-II and chance constrained programming, International Journal of Electrical Power and Energy Systems 74 (2016) 187–194. doi:10.1016/j.ijepes.2015.07.007.
URL http://dx.doi.org/10.1016/j.ijepes.2015.07.007

[54] J. C. Rojas-Zerpa, J. M. Yusta, Application of multicriteria decision methods for electric supply planning in rural and remote areas, Renewable and Sustainable Energy Reviews 52 (2015) 557–571. doi:10.1016/j.rser.2015.07.139.
URL http://dx.doi.org/10.1016/j.rser.2015.07.139

[55] N. Martín-Chivelet, Photovoltaic potential and land-use estimation methodology, Energy 94 (2016) 233–242. doi:10.1016/j.energy.2015.10.108.
URL http://dx.doi.org/10.1016/j.energy.2015.10.108

[56] J. J. Cartelle Barros, M. Lara Coira, M. P. de la Cruz López, A. del Caño Gochi, Comparative analysis of direct employment generated by

renewable and non-renewable power plants, Energy 139 (2017) 542–554. doi:10.1016/j.energy.2017.08.025.

[57] C. O. Henriques, D. H. Coelho, N. L. Cassidy, Employment impact assessment of renewable energy targets for electricity generation by 2020—An IO LCA approach, Sustainable Cities and Society 26 (2016) (2016) 519–530. doi:10.1016/j.scs.2016.05.013.
URL http://dx.doi.org/10.1016/j.scs.2016.05.013

[58] Institute for Sustainable Futures, Calculating global energy sector jobs 2015 methodology update (2015) 1–48.
URL https://opus.lib.uts.edu.au/bitstream/10453/43718/1/Rutovitzetal2015Calculatingglobalenergysectorjobsmethodology.pdf

[59] A. Okunlola, O. Evbuomwan, H. Zaheer, J. Winklmaier, Assessment of Decentralized Hybrid Mini-grids in Sub-Saharan Africa: Market Analysis, Least-Cost Modelling, and Job Creation Analysis, in: Africa-EU Renewable Energy Research and Innovation Symposium 2018, 2018, pp. 21–34.
URL https://www.springer.com/gp/book/9783319934372

[60] X. Luo, J. Wang, M. Dooner, J. Clarke, Overview of current development in electrical energy storage technologies and the application potential in power system operation, Applied Energy 137 (2015) 511–536. doi:10.1016/j.apenergy.2014.09.081.
URL http://dx.doi.org/10.1016/j.apenergy.2014.09.081

[61] P. Haidl, A. Buchroithner, B. Schweighofer, M. Bader, H. Wegleiter, Lifetime analysis of energy storage systems for sustainable transportation, Sustainability 11 (23) (2019). doi:10.3390/su11236731.
URL https://doi.org/10.3390/su11236731

[62] M. Moncecchi, C. Brivio, S. Mandelli, M. Merlo, Battery energy storage systems in microgrids: Modeling and design criteria, Energies 13 (8) (2020) 1–18. doi:10.3390/en13082006.